Lecture #16

- Wiener Filters
- Constrained Least Squares Filter
- Computed Tomography Basics
- Reconstruction and the Radon Transform
- Fourier Slice Theorem
- Filtered Backprojections
- Fan Beams

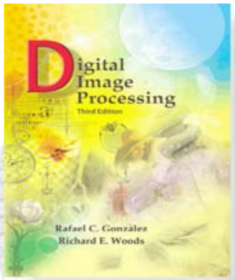

Motion Blurring

Model motion in x- and y-directions over a period T for an integrating detector such as a camera.

$$g(x,y)=\int_0^T f\left[x-x_0(t),y-y_0(t)\right]dt$$

Fourier transform g(x,y) and reverse order of integration

$$G(u,v)=\int_{-\infty}^{\infty}\int_{-\infty}^{\infty} g(x,y)e^{-j2\pi(ux+vy)}dxdy$$

$$=\int_{-\infty}^{\infty}\int_{-\infty}^{\infty}\left[\int_0^T f\left[x-x_0(t),y-y_0(t)\right]dt\right]e^{-j2\pi(ux+vy)}dxdy$$

$$G(u,v)=\int_0^T\left[\int_{-\infty}^{\infty}\int_{-\infty}^{\infty} f\left[x-x_0(t),y-y_0(t)\right]e^{-j2\pi(ux+vy)}dxdy\right]dt$$

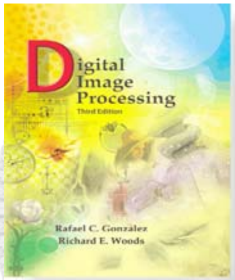

Motion Blurring

Replace innter term by F(u,v), the Fourier transform of f(x,y)

$$G(u,v)=\int_0^T\left[F(u,v)e^{-j2\pi\left(ux_0(t)+vy_0(t)\right)}dxdy\right]dt=F(u,v)\int_0^T e^{-j2\pi\left(ux_0(t)+vy_0(t)\right)}dt$$

Identify the motion blurring transfer function as

$$H(u,v)=\int_0^T e^{-j2\pi\left(ux_0(t)+vy_0(t)\right)}dt$$

We can then model motion degradation as

$$G(u,v)=H(u,v)F(u,v)$$

Where, for $x_0(t)=at/T$, $y_0(t)=0$

$$H(u,v)=\int_0^T e^{-j2\pi ux_0(t)}dt=\int_0^T e^{-j2\pi u\frac{at}{T}}dt=\frac{T}{\pi ua}\sin(\pi ua)e^{-j\pi ua}$$

Modeling Image Degradation

Original image (1st edition cover)

Motion blurring with a=b=0.1 and T=1

FIGURE 5.26 (a) Original image. (b) Result of blurring using the function in Eq. (5.6-11) with $a = b = 0.1$ and $T = 1$.

Motion blurring transfer function

$$H(u,v) = \frac{T}{\pi(ua+vb)} \sin\left[\pi(ua+vb)\right] e^{-j\pi(ua+vb)}$$

Inverse Filtering

- If degraded image is given by degradation + noise

$$G(u,v) = H(u,v)F(u,v) + N(u,v)$$

- Estimate the image by dividing by the degradation function H(u,v)

$$\tilde{F}(u,v) = \frac{G(u,v)}{H(u,v)} = \frac{H(u,v)F(u,v) + N(u,v)}{H(u,v)} = F(u,v) + \frac{N(u,v)}{H(u,v)}$$

We can never recover F(u,v) exactly:

1. N(u,v) is not known since $\eta(x,y)$ is a r.v. — estimated
2. If H(u,v) ->0 then noise term will dominate. Helped by restricting analysis to (u,v) near origin.

Modeling of Degradation

Eq. (5.7-1). (a) Result of using the full filter. (b) Result with H cut off outside a radius of 40; (c) outside a radius of 70; and (d) outside a radius of 85.

$$\tilde{F}(u,v) = F(u,v) + \frac{N(u,v)}{H(u,v)} \quad where \quad H(u,v) = e^{-k\left[\left(u-\frac{M}{2}\right)^2 + \left(v-\frac{N}{2}\right)^2\right]^{\frac{5}{6}}}$$

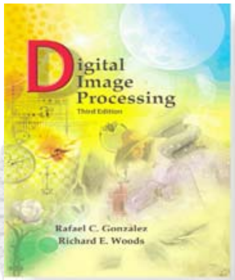

Wiener Filter

Minimize $e^2 = E\left\{\left(f - \hat{f}\right)^2\right\}$

Assuming: 1. f and n are uncorrelated
2. f and/or n is zero mean
3. gray levels in f are a linear function of the gray levels in f

The best estimate $\hat{F}(u,v)$ is then given by

$$\hat{F}(u,v) = \left[\frac{H^*(u,v)S_f(u,v)}{S_f(u,v)\left|H(u,v)\right|^2 + S_\eta(u,v)}\right]G(u,v) = \left[\frac{H^*(u,v)}{\left|H(u,v)\right|^2 + \dfrac{S_\eta(u,v)}{S_f(u,v)}}\right]G(u,v)$$

$$\hat{F}(u,v) = \left[\frac{1}{H(u,v)}\frac{\left|H(u,v)\right|^2}{\left|H(u,v)\right|^2 + \dfrac{S_\eta(u,v)}{S_f(u,v)}}\right]G(u,v)$$

H(u,v) = degradation function
H*(u,v) = complex conjugate of H
|H(u,v)|= H*(u,v) H(u,v)
S_η(u,v)=|N(u,v)|^2=power spectrum of noise (estimated)
S_f(u,v)=|F(u,v)|^2=power spectrum of original image (not known)

Modeling of Degradation

a b c

FIGURE 5.28 Comparison of inverse and Wiener filtering. (a) Result of full inverse filtering of Fig. 5.25(b). (b) Radially limited inverse filter result. (c) Wiener filter result.

Inverse filtering

$$\frac{N(u,v)}{H(u,v)}$$

Radially limit at D_0=75

Wiener filtering

$$\hat{F}(u,v)=\left[\frac{1}{H(u,v)}\frac{|H(u,v)|^2}{|H(u,v)|^2+K}\right]G(u,v)$$

In practice we don't know the power spectrum $S_f(u,v)=|F(u,v)|^2$ of the original image so we replace the S_η/S_f term with a constant K which we vary

Modeling of Degradation

Inverse filtering w/o noise modeling

Wiener filtering w/ noise modeling

Image + motion blur + Gaussian noise (σ^2=650)

Reduce σ^2 to 65

Reduce σ^2 to 0.00650

FIGURE 5.29 (a) 8-bit image corrupted by motion blur and additive noise. (b) Result of inverse filtering. (c) Result of Wiener filtering. (d)–(f) Same sequence, but with noise variance one order of magnitude less. (g)–(i) Same sequence, but noise variance reduced by five orders of magnitude from (a). Note in (h) how the deblurred image is quite visible through a “curtain” of noise.

Constrained Least Squares Filter

$$\underline{g} = \underline{H}\underline{f} + \underline{\eta}$$

g = [$g_{row1}(x,y)$ $g_{row2}(x,y)$ $g_{roww}(x,y)$ . . . $g_{rowN}(x,y)$]
f, η have the same form and dimensions as g, i.e., MNx1
H has dimensions MNxMN which is VERY large

Mininize smoothness

$$C = \sum_{x=0}^{M-1} \sum_{y=0}^{N-1} \left[\nabla^2 f(x,y) \right]^2$$

constraint

$$\left\| \underline{g} - \underline{H}\underline{\hat{f}} \right\| = \left\| \underline{\eta} \right\|^2 = \underline{\eta}^T \underline{\eta}$$

Solution
(Castleman, 1996)

$$\hat{F}(u,v) = \left[\frac{H^*(u,v)}{\left|H(u,v)\right|^2 + \gamma \left|P(u,v)\right|^2} \right] G(u,v)$$

$$P(u,v) = \mathcal{F}\left[p(x,y) \right] \qquad p(x,y) = \begin{bmatrix} 0 & -1 & 0 \\ -1 & 4 & -1 \\ 0 & -1 & 0 \end{bmatrix}$$

Constrained Least Square Filter

Image + motion blur + Gaussian noise (σ^2=650)

Reduce σ^2 to 65

Reduce σ^2 to 0.00650

a b c

FIGURE 5.30 Results of constrained least squares filtering. Compare (a), (b), and (c) with the Wiener filtering results in Figs. 5.29(c), (f), and (i), respectively.

Does a nice job of removing motion degradation <u>and</u> noise

Constrained Least Square Filter

a b

FIGURE 5.31 (a) Iteratively determined constrained least squares restoration of Fig. 5.16(b), using correct noise parameters. (b) Result obtained with wrong noise parameters.

Correct noise parameters

Wrong noise parameters

γ can be determined interactively but the optimum value of γ can be determined from the mean and variance of the noise. Knowing the correct noise parameters is important to the process.

Computed Tomography

1. Forward projection from a source through an absorber to a linear detector array

2. Backproject the signal back to the source to reconstruct the absorber

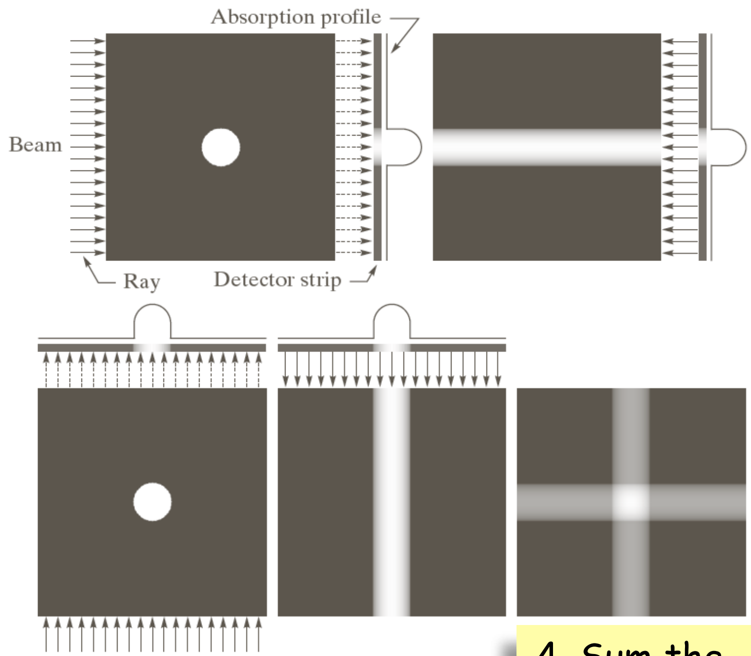

3. Rotate the source and detector array 90° and measure a new forward projection through the same absorber

4. Sum the two back projections to reconstruct a better image of the absorber

a b
c d e

FIGURE 5.32 (a) Flat region showing a simple object, an input parallel beam, and a detector strip. (b) Result of back-projecting the sensed strip data (i.e., the 1-D absorption profile). (c) The beam and detectors rotated by 90°. (d) Back-projection. (e) The sum of (b) and (d). The intensity where the back-projections intersect is twice the intensity of the individual back-projections.

Reconstruction of a Single Object

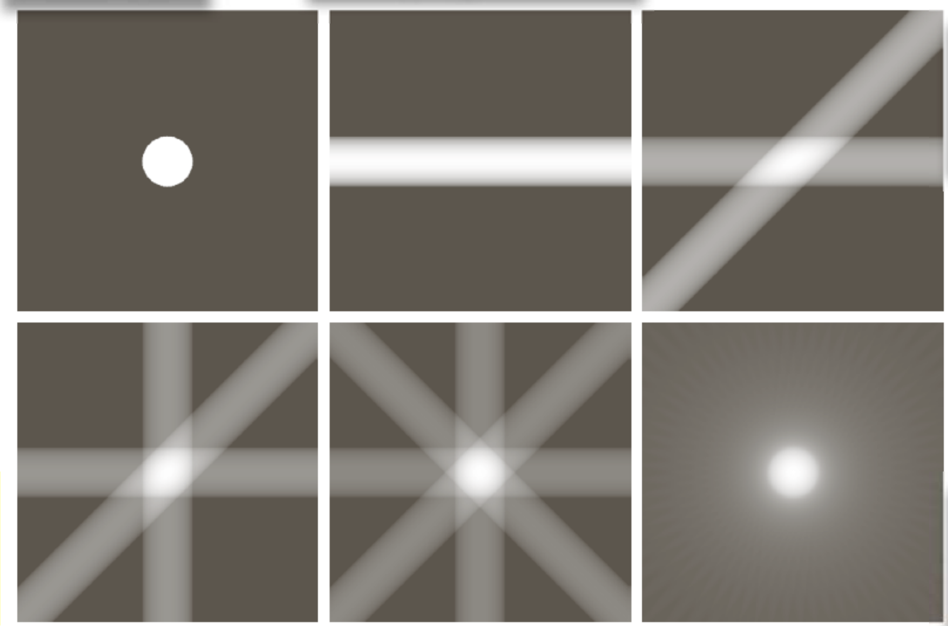

a b c
d e f

FIGURE 5.33 (a) Same as Fig. 5.32(a). (b)–(e) Reconstruction using 1, 2, 3, and 4 backprojections 45° apart. (f) Reconstruction with 32 backprojections 5.625° apart (note the blurring).

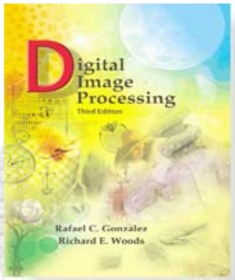

Reconstruction of Multiple Objects

Darker because forward projection was only through smaller less highly absorbing object

Brightest because most absorption — projection was through both absorbing objects

Large highly absorbing object

Smaller less highly absorbing object

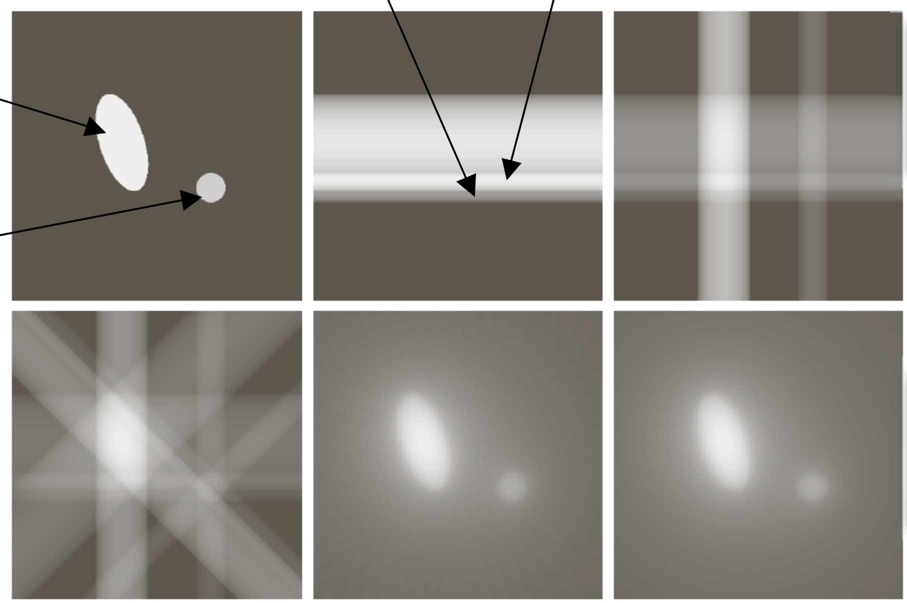

Reconstruction using 2 backprojections 90° apart

Reconstruction using 64 backprojections 2.8125° apart

Reconstruction using 3 backprojections 45° apart

a b c
d e f

Reconstruction using 32 backprojections 5.625° apart

FIGURE 5.34 (a) A region with two objects. (b)–(d) Reconstruction using 1, 2, and 4 backprojections 45° apart. (e) Reconstruction with 32 backprojections 5.625° apart. (f) Reconstruction with 64 backprojections 2.8125° apart.

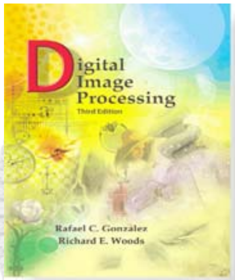

Computed Tomography

G1: Pencil beam, single source and detector — move detector source pair

G2: Narrow fan beam, single source, small linear detector array — move detector source pair (not as much movement required)

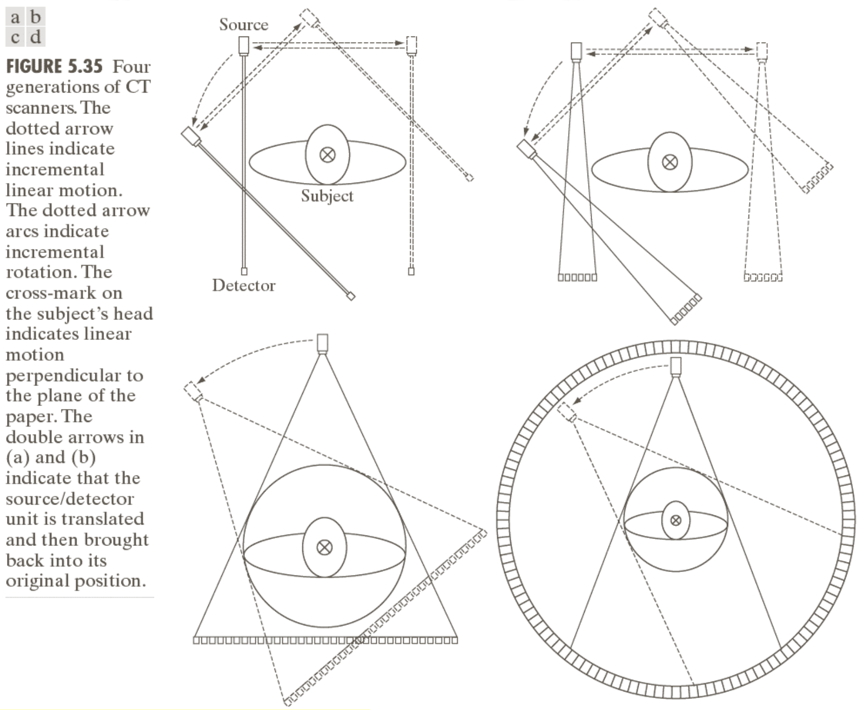

FIGURE 5.35 Four generations of CT scanners. The dotted arrow lines indicate incremental linear motion. The dotted arrow arcs indicate incremental rotation. The cross-mark on the subject's head indicates linear motion perpendicular to the plane of the paper. The double arrows in (a) and (b) indicate that the source/detector unit is translated and then brought back into its original position.

G5: G4 with electromagnetically aimed sources to eliminate mechanical movement

G6: patient moves linearly through rotation scanner describing a helical scan

G7: multi-slice scanners with thick fan beams and 2-D detector arrays

G3: Wide fan beam, single source, large linear detector array — move detector source pair (not as much movement required)

G4: Wide fan beam, rotating source, circular detector array — move source around circle

Basics of the Radon Transform

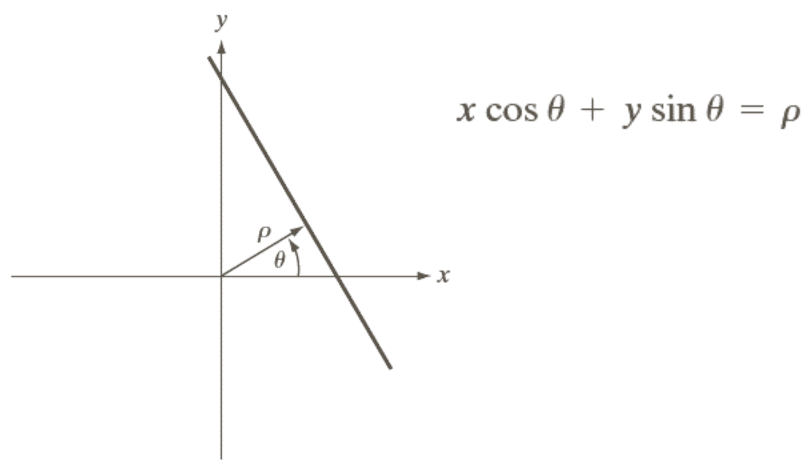

FIGURE 5.36 Normal representation of a straight line.

Describe a line in (x,y) coordinates as:

$$\delta\left(x\cos\theta + y\sin\theta - \rho\right)$$

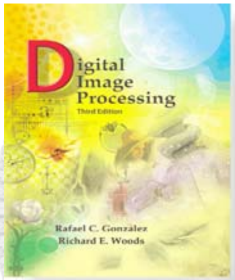

Basics of the Radon Transform

FIGURE 5.37
Geometry of a parallel-ray beam.

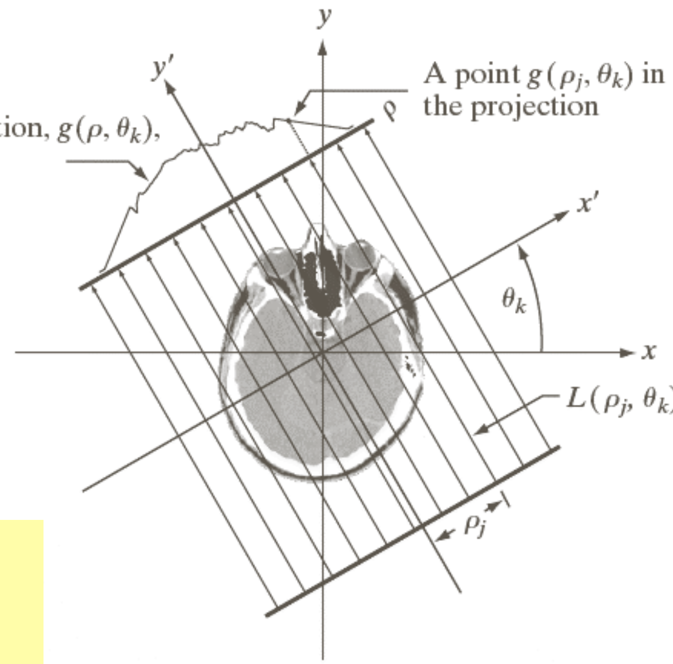

The Radon transform is the line integral (projection) of f(x,y) along a line at an angle θ

$$\mathcal{R}\{f(x,y)\} = g(\rho,\theta) = \int_{-\infty}^{+\infty}\int_{-\infty}^{+\infty} f(x,y)\,\delta(x\cos\theta + y\sin\theta - \rho)\,dxdy$$

Basics of the Radon Transform

$$f(x,y)=\begin{cases} A & x^2+y^2\le r^2 \\ 0 & otherwise \end{cases}$$

Since the absorber is circularly symmetric we only need to do the projection for θ=0°

$$g(\rho,0^\circ)=\int_{-\infty}^{+\infty}\int_{-\infty}^{+\infty} f(x,y)\,\delta(x-\rho)\,dx\,dy$$

$$=\int_{-\infty}^{+\infty} f(\rho,y)\,dy=\int_{-\sqrt{r^2-\rho^2}}^{+\sqrt{r^2-\rho^2}} A\,dy$$

$$=\begin{cases} 2A\sqrt{r^2-\rho^2} & |\rho|\le r \\ 0 & otherwise \end{cases}$$

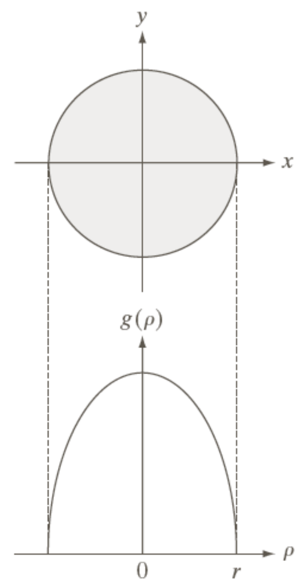

FIGURE 5.38 A disk and a plot of its Radon transform, derived analytically. Here we were able to plot the transform because it depends only on one variable. When g depends on both ρ and θ, the Radon transform becomes an image whose axes are ρ and θ, and the intensity of a pixel is proportional to the value of g at the location of that pixel.

$$g(\rho,\theta)=\begin{cases} 2A\sqrt{r^2-\rho^2} & |\rho|\le r \\ 0 & otherwise \end{cases}$$

This is the Radon transform g(ρ) for θ=0°

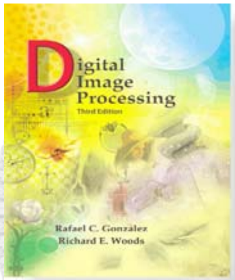

Sinograms

The plot of $g(\rho,\theta)$ as an intensity with ρ on the horizontal and θ on the vertical is called a sinogram.

The Shepp-Logan phantom is designed to simulate the absorption of a brain with small tumors

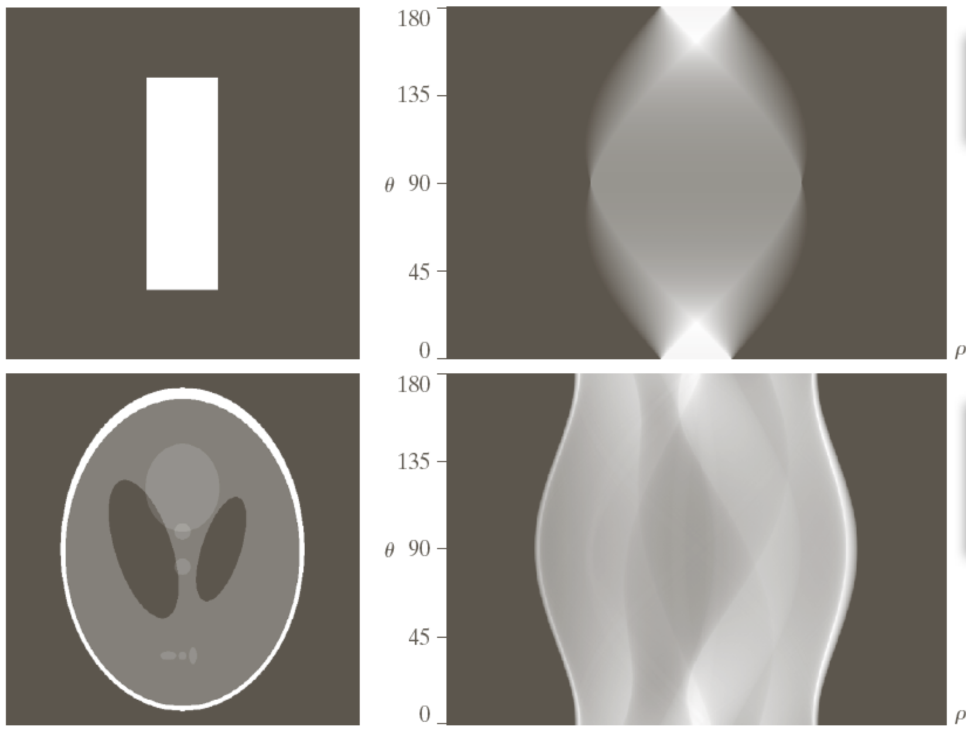

The sinogram of a bar.

The sinogram of the Shepp-Logan phantom.

a b
c d

FIGURE 5.39 Two images and their sinograms (Radon transforms). Each row of a sinogram is a projection along the corresponding angle on the vertical axis. Image (c) is called the *Shepp-Logan phantom*. In its original form, the contrast of the phantom is quite low. It is shown enhanced here to facilitate viewing.

Backprojection of Sinograms

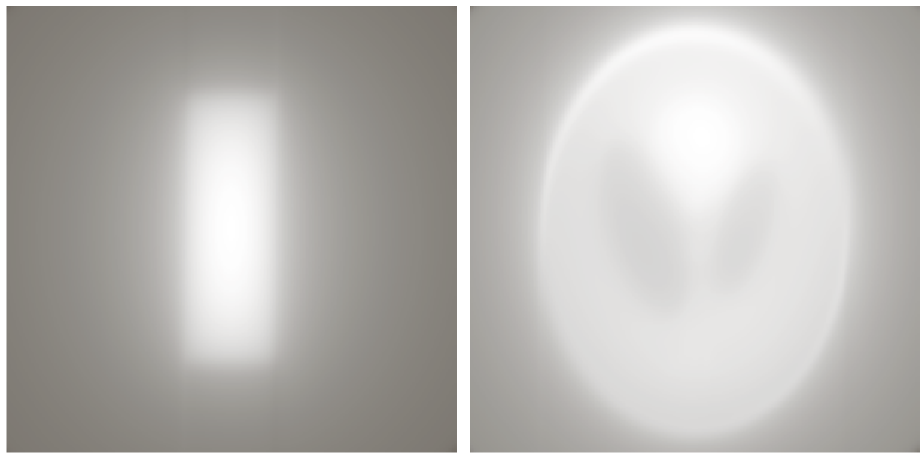

a b

FIGURE 5.40 Backprojections of the sinograms in Fig. 5.39.

There is significant blurring using this approach

The backprojection for a specific angle θ is the line

$$f_\theta(x,y) = g(x\cos\theta + y\sin\theta, \theta)$$

The complete reconstruction is the integral over all θ

$$f(x,y) = \int_0^\pi f_\theta(x,y)\,d\theta$$

Fundamental CT Reconstruction

- Physically measure the projection
- Back project each projection
- Sum all the projections to generate one image
- Results in blurred images

Fourier Slice Theorem

$$G(\omega,\theta)=\int_{-\infty}^{+\infty} g(\rho,\theta)e^{-j2\pi\omega\rho}d\rho$$

Compute the 1-D Fourier transform of g(ρ,θ)

$$G(\omega,\theta)=\int_{-\infty}^{+\infty}\int_{-\infty}^{+\infty}\int_{-\infty}^{+\infty} f(x,y)\delta(x\cos\theta+y\sin\theta-\rho)dxdye^{-j2\pi\omega\rho}d\rho$$

Substitute the expression for the projection g(ρ,θ)

$$G(\omega,\theta)=\int_{-\infty}^{+\infty}\int_{-\infty}^{+\infty} f(x,y)\left[\int_{-\infty}^{+\infty}\delta(x\cos\theta+y\sin\theta-\rho)e^{-j2\pi\omega\rho}d\rho\right]dxdy$$

Reverse the order of integration and evaluate

$$G(\omega,\theta)=\int_{-\infty}^{+\infty}\int_{-\infty}^{+\infty} f(x,y)e^{-j2\pi\omega(x\cos\theta+y\sin\theta)}dxdy$$

This is the Fourier transform of the absorption f(x,y) evaluated at u=ωcosθ; v=ωsinθ

$$G(\omega,\theta)=\left[\int_{-\infty}^{+\infty}\int_{-\infty}^{+\infty} f(x,y)e^{-j2\pi(ux+vy)}dxdy\right]_{u=\omega\cos\theta;v=\omega\sin\theta}$$

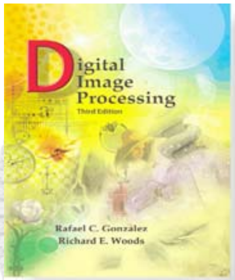

Fourier Slice Theorem

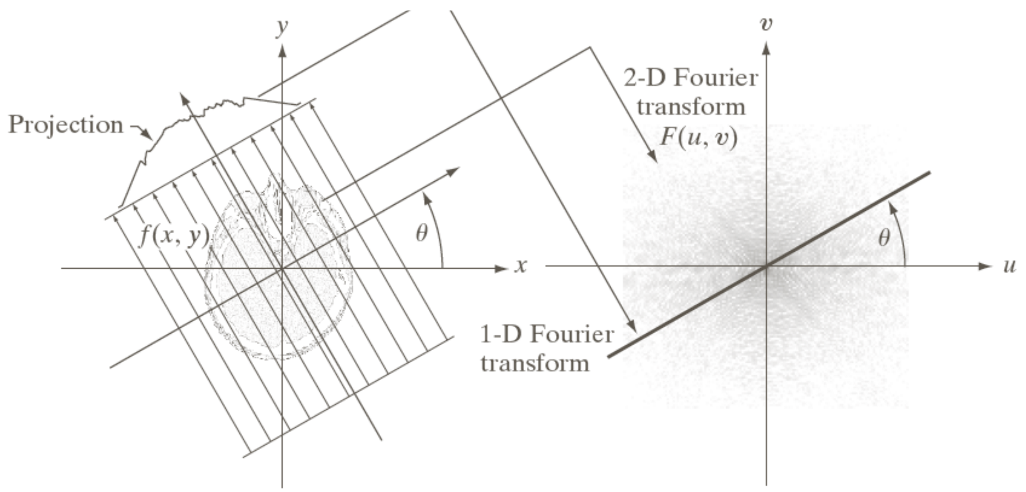

FIGURE 5.41 Illustration of the Fourier-slice theorem. The 1-D Fourier transform of a projection is a slice of the 2-D Fourier transform of the region from which the projection was obtained. Note the correspondence of the angle θ.

$$G(\omega,\theta) = \left[F(u,v)\right]_{u=\omega\cos\theta;\, v=\omega\sin\theta}$$
$$= F(\omega\cos\theta, \omega\sin\theta)$$

The Fourier transform of a projection is a slice of the 2-D Fourier transform of the density f(x,y)

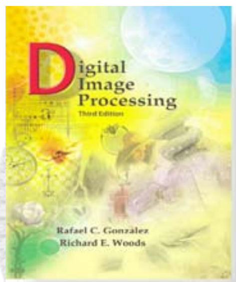

Reconstruction Using the Fourier Slice Theorem

$$f(x,y)=\int_{-\infty}^{+\infty}\int_{-\infty}^{+\infty}F(u,v)e^{j2\pi(ux+vy)}dudv$$

The inverse 2-D Fourier transform of F(u,v)

$$f(x,y)=\int_{0}^{2\pi}\int_{0}^{\infty}F(\omega\cos\theta,\omega\sin\theta)e^{j2\pi\omega(x\cos\theta+y\sin\theta)}\omega d\omega d\theta$$

Rewrite in polar coordinates

$$f(x,y)=\int_{0}^{2\pi}\int_{0}^{\infty}G(\omega,\theta)e^{j2\pi\omega(x\cos\theta+y\sin\theta)}\omega d\omega d\theta$$

Use the Fourier Slice Theorem to recognize G(ω,θ)

$$f(x,y)=\int_{0}^{\pi}\int_{0}^{\infty}G(\omega,\theta)e^{j2\pi\omega(x\cos\theta+y\sin\theta)}\omega d\omega d\theta+\int_{\pi}^{2\pi}\int_{0}^{\infty}G(\omega,\theta)e^{j2\pi\omega(x\cos\theta+y\sin\theta)}\omega d\omega d\theta$$

Separate

$$f(x,y)=\int_{0}^{\pi}\int_{0}^{\infty}G(\omega,\theta)e^{j2\pi\omega(x\cos\theta+y\sin\theta)}\omega d\omega d\theta+\int_{0}^{\pi}\int_{0}^{\infty}G(-\omega,\theta)e^{j2\pi\omega(x\cos\theta+y\sin\theta)}\omega d\omega d\theta$$

Use symmetry

$$f(x,y)=\int_{0}^{\pi}\int_{0}^{\infty}|\omega|G(\omega,\theta)e^{j2\pi\omega(x\cos\theta+y\sin\theta)}d\omega d\theta$$

Recombine

$$f(x,y)=\int_{0}^{\pi}\left[\int_{0}^{\infty}|\omega|G(\omega,\theta)e^{j2\pi\omega\rho}d\omega\right]_{\rho=x\cos\theta+y\sin\theta}d\theta$$

Rearrange

Reconstruction Using the Fourier Slice Theorem

$$f(x,y)=\int_0^{\pi}\left[\int_0^{\infty}|\omega|G(\omega,\theta)e^{j2\pi\omega\rho}d\omega\right]_{\rho=x\cos\theta+y\sin\theta}d\theta$$

The inner term is a 1-D inverse Fourier transform.

The $|\omega|$ is a ramp filter (whose inverse Fourier transform does not exist since it is not bounded) modifying the transform.

In practice we multiply $|\omega|$ by another filter, a windowing function, which limits its high frequency response.

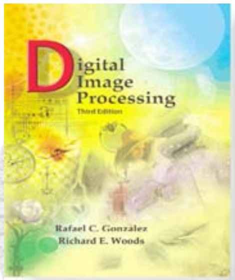

Filtered Backprojections

|ω| multiplied by a box function in the frequency domain.

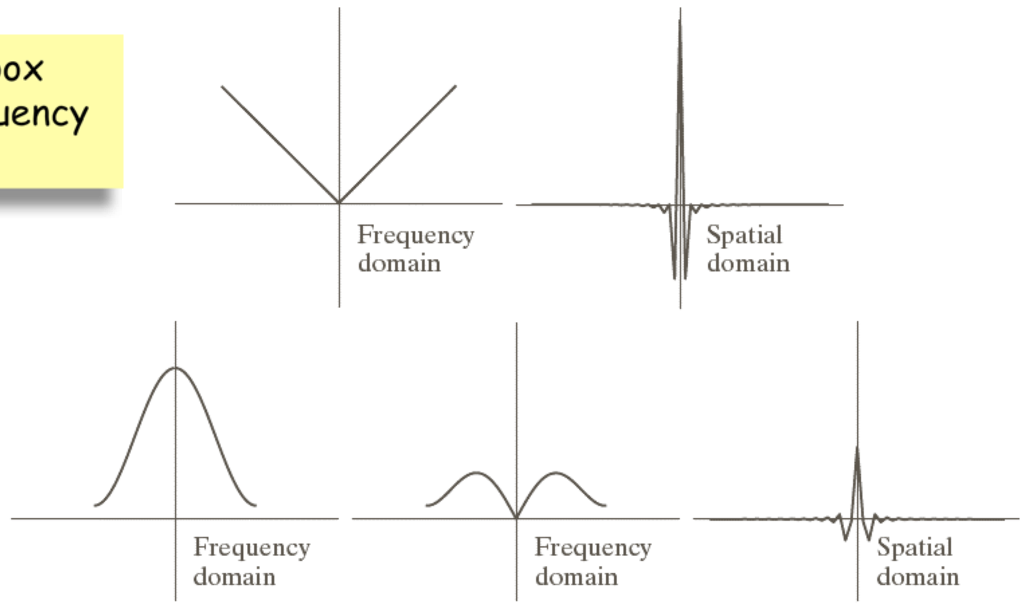

a b
c d e

FIGURE 5.42 (a) Frequency domain plot of the filter $|\omega|$ after band-limiting it with a box filter. (b) Spatial domain representation. (c) Hamming windowing function. (d) Windowed ramp filter, formed as the product of (a) and (c). (e) Spatial representation of the product (note the decrease in ringing).

Hamming window function

Hamming filtered |ω| and its inverse Fourier transform

Reconstruction Using Filtered Backprojections

- Physically measure the projection for angle θ_k
- Compute the 1-D Fourier Transform of each projection
- Multiply each Fourier Transform by the filter function $|\omega|$ and an appropriate window, e.g., Hamming
- Obtain the inverse 1-D Fourier Transform of the windowed, filtered transform
- Integrate (sum) all the 1-D transforms to generate one image

Filtered Backprojection

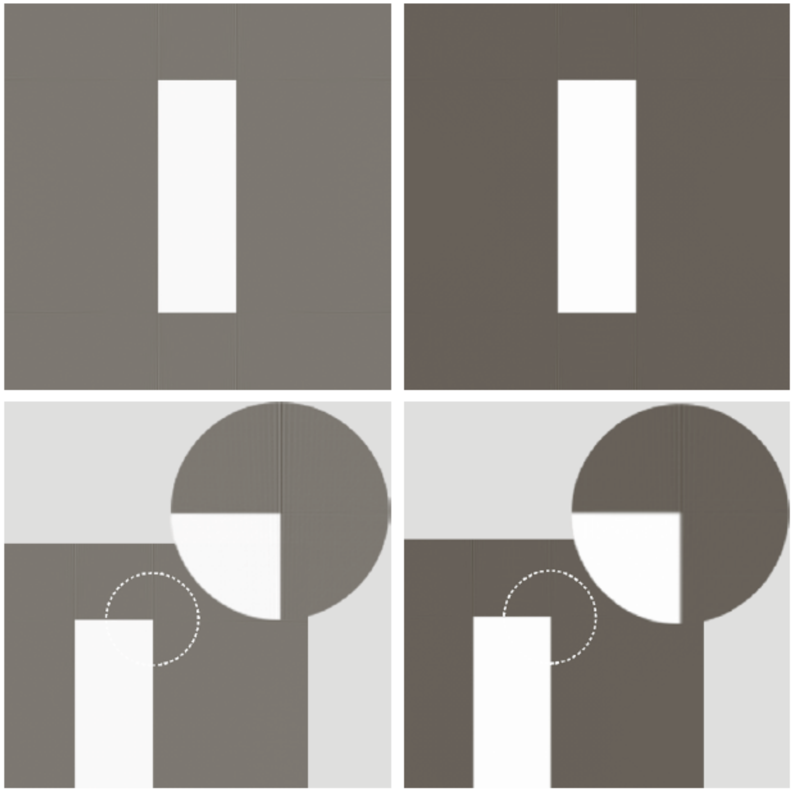

a b
c d

FIGURE 5.43 Filtered backprojections of the rectangle using (a) a ramp filter, and (b) a Hamming-windowed ramp filter. The second row shows zoomed details of the images in the first row. Compare with Fig. 5.40(a).

Backprojection filtered by a ramp filter.

Backprojection filtered by a Hamming-windowed ramp filter.

Filtered Backprojection

a b

FIGURE 5.44 Filtered backprojections of the head phantom using (a) a ramp filter, and (b) a Hamming-windowed ramp filter. Compare with Fig. 5.40(b).

Backprojection filtered by a ramp filter.

Backprojection filtered by a Hamming-windowed ramp filter.

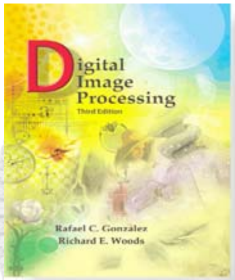

Computed Tomography

To analyze the fan-beam geometry for G4 and later machines we switch from frequency domain analysis to convolution.

$$f(x,y)=\int_0^{\pi}\left[\int_{-\infty}^{\infty}|\omega|G(\omega,\theta)e^{j2\pi\omega\rho}d\omega\right]_{\rho=x\cos\theta+y\sin\theta}d\theta$$

$$f(x,y)=\int_0^{\pi}\left[s(\rho)\star g(\rho,\theta)\right]_{\rho=x\cos\theta+y\sin\theta}d\theta$$

$$f(x,y)=\int_0^{\pi}\left[\int_{-\infty}^{\infty}g(\rho,\theta)s(x\cos\theta+y\sin\theta-\rho)d\rho\right]_{\rho=x\cos\theta+y\sin\theta}d\theta$$

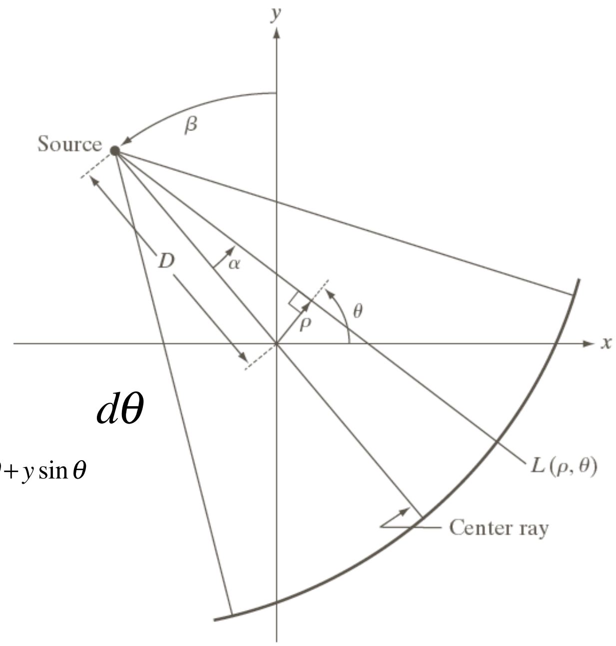

FIGURE 5.45 Basic fan-beam geometry. The line passing through the center of the source and the origin (assumed here to be the center of rotation of the source) is called the *center ray*.

This is a convolution of the ramp filter and the corresponding projection

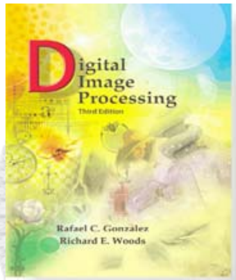

Computed Tomography

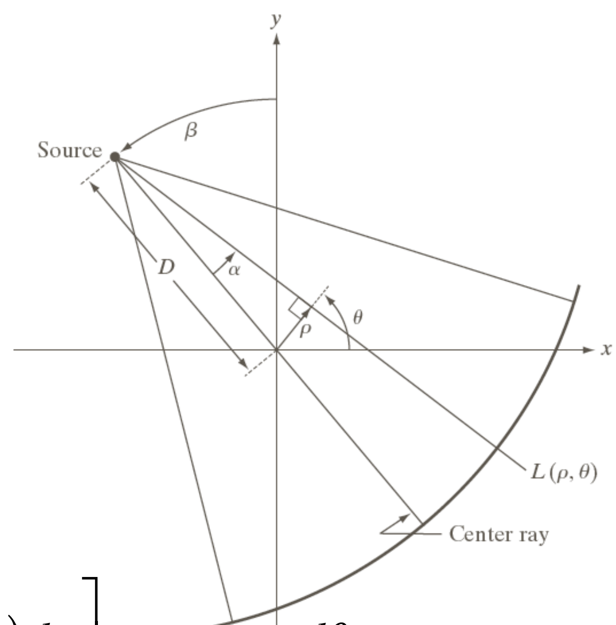

FIGURE 5.45 Basic fan-beam geometry. The line passing through the center of the source and the origin (assumed here to be the center of rotation of the source) is called the *center ray*.

$$f(x,y)=\int_0^{\pi}\left[\int_{-\infty}^{\infty} g(\rho,\theta)s(x\cos\theta+y\sin\theta-\rho)\,d\rho\right]_{\rho=x\cos\theta+y\sin\theta} d\theta$$

$$f(x,y)=\frac{1}{2}\int_0^{2\pi}\int_{-T}^{T}\int_{-\infty}^{\infty} g(\rho,\theta)s(x\cos\theta+y\sin\theta-\rho)\,d\rho\, d\theta$$

We recognize that the projections are mirror images and then convert to polar coordinates

Computed Tomography

We recognize that the projections are mirror images and then convert to polar coordinates

$$Let\ \ x = r\cos\varphi\ \ and\ \ y = r\sin\varphi$$

$$Then\ x\cos\theta + y\sin\theta =$$

$$r\cos\varphi\cos\theta + r\sin\varphi\sin\theta = r\cos(\theta-\varphi)$$

$$f(x,y) = \frac{1}{2}\int_{0}^{2\pi}\int_{-T}^{T} g(\rho,\theta)s\left[r\cos(\theta-\alpha)-\rho\right]d\rho d\theta$$

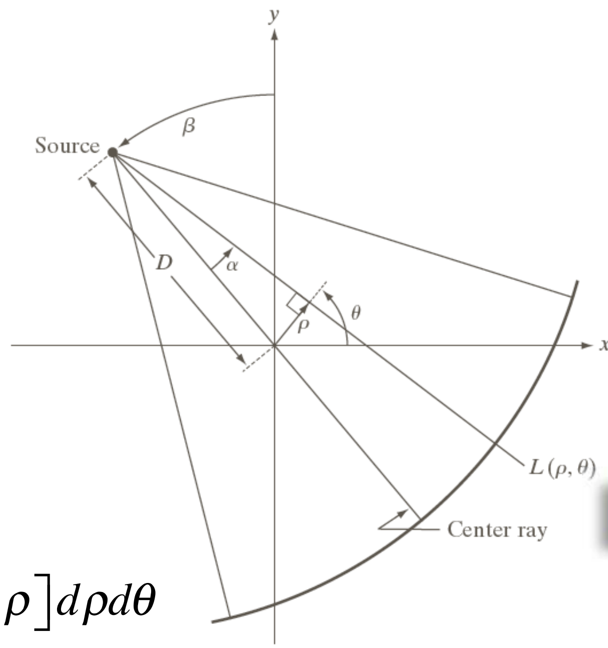

FIGURE 5.45 Basic fan-beam geometry. The line passing through the center of the source and the origin (assumed here to be the center of rotation of the source) is called the *center ray*.

For this beam geometry

$$\theta = \beta + \alpha$$

$$\rho = \sin\alpha$$

Using this information we then transform the variables of integration to α and β

$$f(x,y) = \frac{1}{2}\int_{-\alpha}^{2\pi-\alpha}\int_{\sin^{-1}\left(-\frac{T}{D}\right)}^{\sin^{-1}\left(\frac{T}{D}\right)} g(D\sin\alpha,\alpha+\beta)s\left[r\cos(\beta+\alpha-\varphi)-S\sin\alpha\right]D\cos\alpha d\alpha d\beta$$

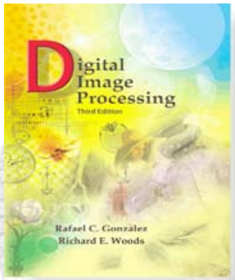

Computed Tomography

Since $-\alpha_m < \alpha < +\alpha_m$ and we can rotate α with no loss of generality

$$f(x,y)=\frac{1}{2}\int_{0}^{2\pi}\int_{-\alpha_m}^{\alpha_m} p(\alpha,\beta)s\left[r\cos(\beta+\alpha-\varphi)-D\sin\alpha\right]D\cos\alpha\, d\alpha\, d\beta$$

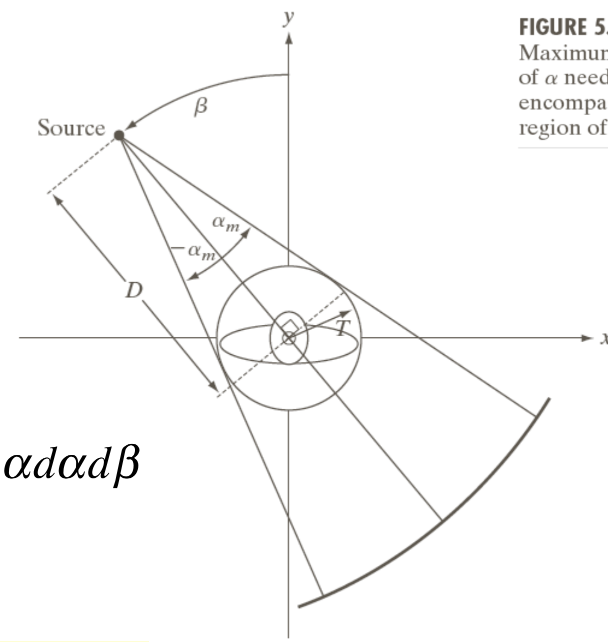

FIGURE 5.46 Maximum value of α needed to encompass a region of interest.

This is the fundamental fan beam reconstruction formula where

$$p(\alpha,\beta)=g(D\sin\alpha,\alpha+\beta)$$

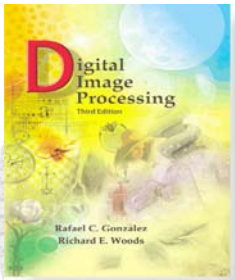

Computed Tomography

From problem 5.33

$$r\cos(\beta+\alpha-\varphi)-D\sin\alpha = R\sin(\alpha'-\alpha)$$

$$f(r,\varphi)=\frac{1}{2}\int_{0}^{2\pi}\int_{-\alpha_m}^{\alpha_m} p(\alpha,\beta)s\left[R\sin(\alpha'+\alpha)\right]D\cos\alpha\, d\alpha\, d\beta$$

From problem 5.34

$$s(R\sin\alpha)=\left(\frac{\alpha}{R\sin\alpha}\right)^2 s(\alpha)$$

$$f(r,\varphi)=\int_{0}^{2\pi}\frac{1}{R^2}\left[\int_{-\alpha_m}^{\alpha_m} q(\alpha,\beta)h[\alpha'-\alpha]\,d\alpha\right]d\beta$$

where $h(\alpha)=\frac{1}{2}\left(\frac{\alpha}{\sin\alpha}\right)^2 s(\alpha)$ and $q(\alpha,\beta)=p(\alpha,\beta)D\cos\alpha$

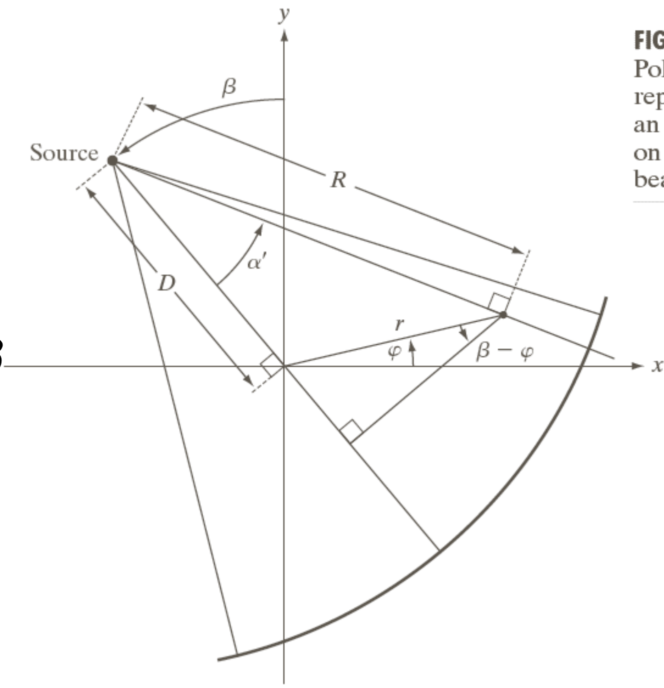

FIGURE 5.47 Polar representation of an arbitrary point on a ray of a fan beam.

Computed Tomography

This is computationally hard to evaluate

$$f(r,\varphi)=\int_0^{2\pi}\frac{1}{R^2}\left[\int_{-\alpha_m}^{\alpha_m} q(\alpha,\beta)h[\alpha'-\alpha]\,d\alpha\right]d\beta$$

A common simplification is

$$p(\alpha,\beta)=g(\rho,\theta)=g(D\cos\alpha,\alpha+\beta)$$

For a discrete system let $\Delta\beta=\Delta\alpha=\gamma$

$$p(n\gamma,m\gamma)=g(D\sin n\gamma,(m+n)\gamma)$$

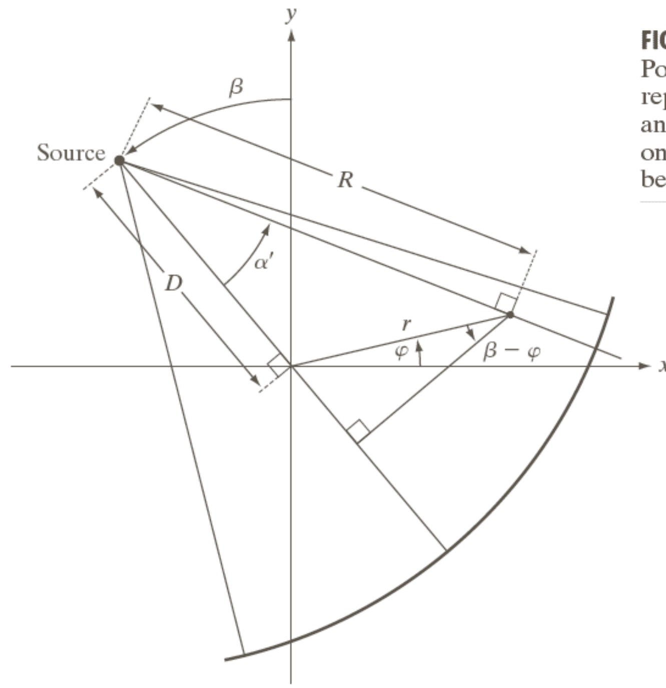

FIGURE 5.47 Polar representation of an arbitrary point on a ray of a fan beam.

Computed Tomography

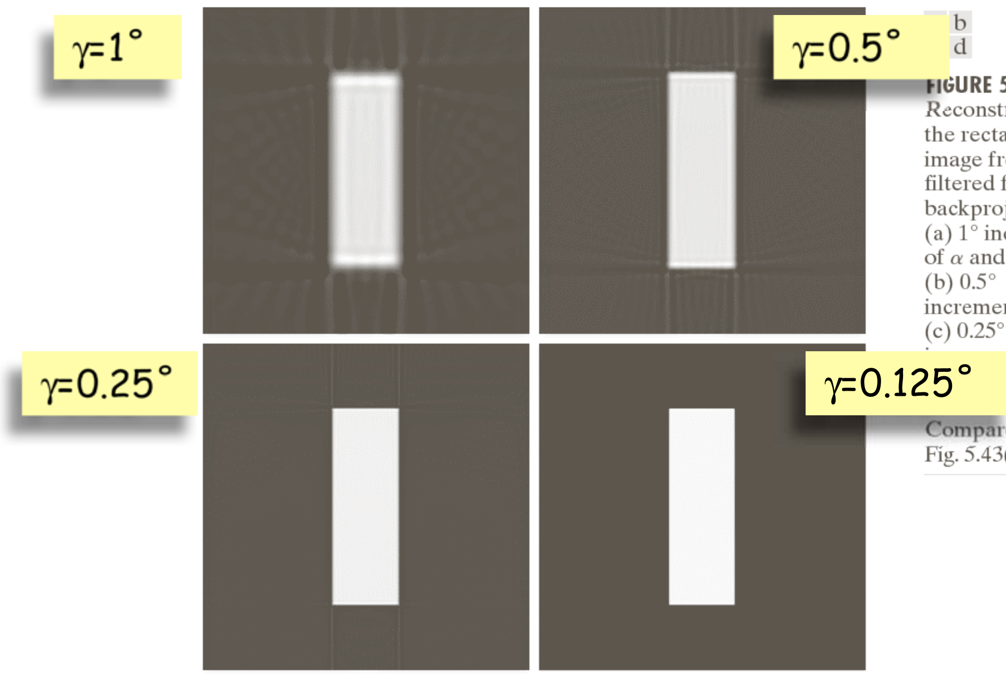

b
d

FIGURE 5.48 Reconstruction of the rectangle image from filtered fan backprojections. (a) 1° increments of α and β. (b) 0.5° increments. (c) 0.25° ts. ts. Compare (d) with Fig. 5.43(b).

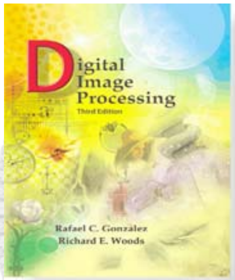

Computed Tomography

γ=1°

γ=0.5°

γ=0.25°

γ=0.125°

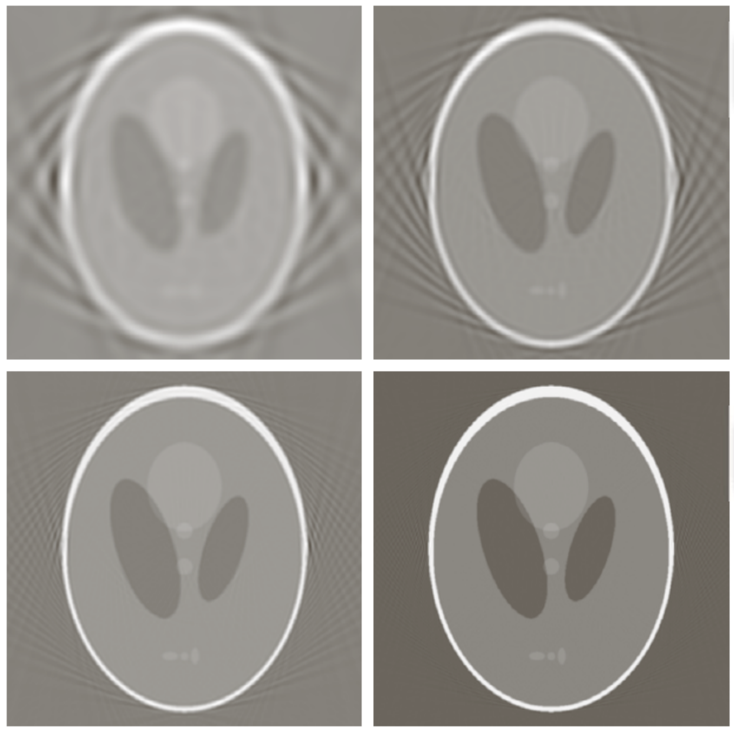

a b

Reconstruction of the head phantom image from filtered fan backprojections. (a) 1° increments of α and β. (b) 0.5° increments. (c) 0.25° increments.

Fig. 5.44(b).